Increased CD8+ T-cell Infiltration and Efficacy for Multikinase Inhibitors After PD-1 Blockade in Hepatocellular Carcinoma

Hiroto Kikuchi, MD, PhD,[1,3] Aya Matsui, PhD,[1] Satoru Morita, MD, PhD,[1] Zohreh Amoozgar, PhD,[1] Koetsu Inoue, MD, PhD,[1] Zhiping Ruan, MD, PhD,[1] Daniel Staiculescu, BSc,[1] Jeffrey Sum-Lung Wong, MBBS,[2] Peigen Huang, MD,[1] Thomas Yau, MD,[2] Rakesh K. Jain, PhD,[1] Dan G. Duda, DMD, PhD 🄳[1,*]

[1]Edwin L. Steele Laboratories for Tumor Biology, Department of Radiation Oncology, Massachusetts General Hospital and Harvard Medical School, Boston, MA, USA and [2]Department of Medicine, Queen Mary Hospital, The University of Hong Kong, Hong Kong, China

[3]Current affiliation: Department of Surgery, Hiratsuka City Hospital, Kanagawa, Japan

*Correspondence to: Dan G. Duda, DMD, PhD, Edwin L. Steele Laboratories for Tumor Biology, Department of Radiation Oncology, Massachusetts General Hospital, 100 Blossom St, Cox-734, Boston, MA 02478, USA (e-mail: gduda@partners.org).

Abstract

Immune checkpoint blockade combined with antiangiogenic therapy induces vascular normalization and antitumor immunity and is efficacious in hepatocellular carcinoma (HCC); but whether and how initial immunotherapy affects the efficacy of subsequent antiangiogenic therapy are unknown. We evaluated a cohort of HCC patients (n = 25) who received the pan–vascular endothelial growth factor receptor multikinase inhibitor sorafenib after initial therapy with an antiprogrammed cell death protein (PD)–1 antibody and found superior outcomes in these patients (12% overall response rate to sorafenib and a median overall survival of 12.1 months). To prove this potential benefit, we examined the impact of an anti–PD-1 antibody on response to subsequent sorafenib treatment in orthotopic models of murine HCC. Prior anti–PD-1 antibody treatment amplified HCC response to sorafenib therapy and increased survival (n = 8-9 mice per group, hazard ratio = 0.28, 95% confidence interval = 0.09 to 0.91; 2-sided *P* = .04). Anti–PD-1 therapy showed angioprotective effects on HCC vessels to subsequent sorafenib treatment, which enhanced the benefit of this therapy sequence in a CD8+ T-cell–dependent manner. This priming approach using immunotherapy provides an immediately translatable strategy for effective HCC treatment while reducing drug exposure.

Hepatocellular carcinoma (HCC) is a frequent liver malignancy and cause of cancer-related death. The outcomes remain poor even with the advent of effective antiangiogenic therapy and, more recently, immune checkpoint blockade (ICB).

Sorafenib, a multikinase inhibitor with anti–vascular endothelial growth factor receptor (VEGFR) 1-3 activity, was the first systemic therapy for advanced HCC (1,2). The pan-VEGFR multikinase inhibitor lenvatinib showed equivalent efficacy with sorafenib, whereas other multikinase inhibitors of VEGFR (regorafenib, cabozantinib) and an anti-VEGFR2 antibody (ramucirumab) showed efficacy post-sorafenib in HCC (3–6). However, tumor responses are rare, adverse effects are frequent, and overall survival (OS) benefits are limited.

HCC usually develops on a background of chronic liver inflammation, often associated with expression of immune checkpoint molecules such as programmed cell death protein (PD)–1 and its ligand programmed death-ligand (PD-L)–1 (7,8). ICB with the anti–PD-1 antibodies nivolumab and pembrolizumab showed promise in phase I and II trials, but phase 3 trials of these agents in monotherapy failed to reach the prespecified survival endpoints as first line or post-sorafenib (9).

However, combining the anti-VEGF antibody bevacizumab with the anti–PD-L1 antibody atezolizumab showed unprecedented efficacy vs sorafenib (10). Based on this favorable treatment interaction, multiple combinations of multikinase inhibitors with anti–PD-1 or anti–PD-L1 antibodies are being tested in clinical trials, with promising initial results indicating feasibility, potential efficacy, and activation of antitumor immunity (11). Unfortunately, prolonged therapy with these agents in combination has the risk of high systemic and financial toxicities, and the response to treatment, although impressive, remains transient in most patients. Thus, the mechanisms

underlying the treatment interaction between antiangiogenics and ICB remain unclear, and how they should be sequenced to improve treatment outcomes, feasibility, and response durability remains unknown (12).

In breast cancer models, effective antitumor immunity reciprocally regulated vascular normalization via $CD4^+$ cell infiltration, including after preventative ICB (13). Moreover, ICB-mediated vascular normalization in HCC is critical for the benefit of this immunotherapy when combined concomitantly with anti-VEGFR2 antibodies or with judiciously dosed multikinase inhibitors (14,15).

The normalizing effect of ICB treatment raises the intriguing possibility of priming effects for subsequent therapies (16–18). Thus, we conducted a retrospective analysis of data from 25 consecutive HCC patients with Child-Pugh A cirrhosis treated with sorafenib after initially receiving off-label anti-PD-1 antibodies (eg, nivolumab, pembrolizumab) at the University of Hong Kong (see Supplementary Material, available online). These HCC patients showed a 12% overall response rate to sorafenib and had a median OS of 12.1 months (Supplementary Figure 1, A and B, available online). The response rate and survival duration in these patients compare favorably with the outcome from the Asia-Pacific phase III trial in Asian patients and even the data from the sorafenib HCC assessment randomized protocol (SHARP trial) in European and Asian HCC patients (1,2), in which responses to sorafenib were exceptionally rare (2%-3%). The higher-than-expected response rate and favorable survival seen in these patients warranted further studies of anti-PD-1 therapy priming in animal models.

Quantitative variables were compared using the Wilcoxon rank sum test. Overall survival distribution was analyzed by Cox proportional hazard model with P values calculated from the log-rank test. The assumption of proportionality was verified by graphical method and goodness-of-fit test. All statistical tests were 2-sided, and a P value less than .05 was considered statistically significant.

To demonstrate that initial anti-PD-1 therapy can enhance the response to standard (high-dose) sorafenib therapy, we used an established preclinical mouse model of orthotopic HCC known to respond to anti-PD-1 therapy (14,15). In line with the benefit suggested by the clinical data, treatment with antimurine PD-1 antibody (clone RMP-014, 3×10 mg/kg, intraperitoneally) for 1 week followed by sorafenib (40 mg/kg daily, orally) (PS group) statistically significantly prolonged median OS in mice when compared with anti-PD-1 treatment followed by control phosphate-buffered saline (PBS) gavage (PC) (hazard ratio [HR] = 0.55, 95% confidence interval [CI] = 0.01 to 0.48; $P = .009$), with sorafenib without anti-PD-1 priming (CS) (HR = 0.28, 95% CI = 0.09 to 0.91; $P = .04$), or with immunoglobulin control (CC) (HR = 0.053, 95% CI = 0.01 to 0.45; $P = .007$) (Figure 1, A and B; Supplementary Figure 1, C and D, available online). Moreover, tumor growth was delayed, and complete responses occurred in 22.2% of the mice in the PS group (Figure 1, A and B). Similar efficacy (ie, delayed tumor growth, durable responses, and increased median OS) was seen with regorafenib after prior anti-PD-1 treatment (Supplementary Figure 2, A and B, available online).

We then repeated the study but sacrificed all mice at day 13 to evaluate the effects of sorafenib treatment after initial anti-PD-1 therapy using immunofluorescence. Anti-PD-1 therapy priming increased the frequency of $CD8^+$ and $CD4^+$ T cells in HCC tissues (Figure 1, C-E). The frequency of infiltrating $CD8^+$ but not $CD4^+$ T cells was increased by subsequent sorafenib therapy (Figure 1, C-E). These findings were confirmed in autochthonous HCCs induced using Cre-adenovirus injection in $Mst1^{-/-}Mst2^{f/-}$ mice (14,19) (Supplementary Figure 2, C-E, available online). To examine the effects of sequential anti-PD-1 therapy followed by sorafenib on HCC vasculature, we measured $CD31^+$ microvessel density (MVD) and α-SMA$^+$ pericyte-covered MVD in tumor samples (Figure 1, F). In contrast to upfront sorafenib, which decreased MVD, sorafenib after anti-PD-1 therapy priming resulted in higher MVD and pericyte-covered MVD (Figure 1, G and H). This effect was confirmed using immunofluorescence in autochthonous HCC model (Supplementary Figure 2, F-H, available online).

To determine whether the increase in $CD8^+$ T cells mediates the benefit of sorafenib after anti-PD-1 therapy priming, we used anti-CD8 antibody-mediated depletion started concomitantly with sorafenib treatment (Supplementary Figure 1, E and F, available online). Sorafenib therapy alone after anti-PD-1 (PS) statistically significantly prolonged OS vs control (C) (HR = 0.10, 95% CI = 0.03 to 0.33; $P < .001$); CD8 depletion at the time of sorafenib initiation (PDS) compromised the survival benefit (PS vs PDS, HR = 0.31, 95% CI = 0.13 to 0.75; $P = .01$) (Figure 2, A). Interestingly, $CD8^+$ cell depletion did not affect the initial growth delay (Figure 2, B). Previous studies demonstrated that $CD4^+$ and $CD8^+$ cells can mediate vascular normalization after effective ICB in breast cancer models (13,20). Our prior work in HCC models demonstrated the role of $CD4^+$ cells in vascular normalization induced by concomitant antibody blockade of VEGFR2 and PD-1 (14). Thus, we conducted a time-matched study to reveal the impact of $CD8^+$ depletion on the effects of sorafenib sequenced after anti-PD-1 therapy in HCC. At day 13, $CD8^+$ cell depletion resulted in almost complete absence of intratumoral $CD8^+$ T cells as well as in reduction in $CD4^+$ T cells (Figure 2, C-E). Moreover, $CD8^+$ cell depletion prevented the increase in MVD after sorafenib post-anti-PD-1 therapy (Figure 2, F-H).

In summary, anti-PD-1 treatment increases $CD4^+$ and $CD8^+$ T-cell infiltration and is angioprotective for subsequent multikinase inhibitor treatment. In this treatment sequence, sorafenib converted into an immune-stimulating agent by promoting $CD8^+$ T-cell infiltration. This approach may address the challenges raised by concomitant combinations of these drugs and has direct implications for de-escalation of therapies for HCC and potentially other cancers.

Funding

Notes

Role of the funders: The funders had no role in the design of the study; the collection, analysis, or interpretation of the data; the writing of the manuscript, or the decision to submit the manuscript for publication.
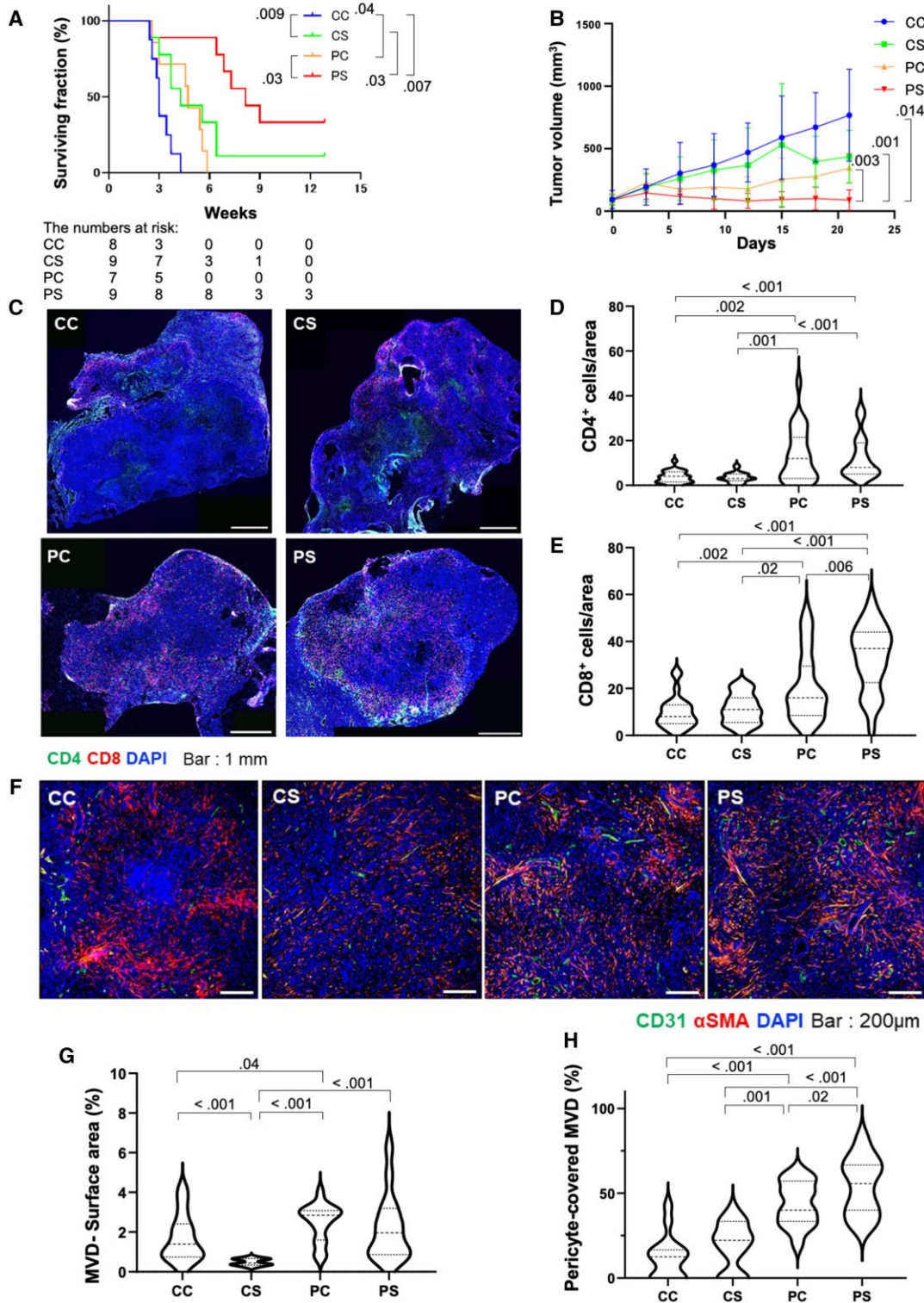
Figure 1. Changes in overall survival, tumor growth kinetics, and intratumoral lymphocyte infiltration and microvascular density in mice receiving sorafenib treatment after prior anti–PD-1 therapy. **A, B)** Kaplan-Meier distributions of overall survival (**A**) and tumor growth kinetics (**B**) in orthotopic HCC-bearing mice receiving sorafenib after initial anti–PD-1 therapy (PS) compared with IgG control followed by PBS gavage (CC), IgG control followed by sorafenib (CS), and anti–PD-1 therapy followed by PBS gavage (PC) (n = 8-9 mice per group). Tumor volume at day 21 was statistically significantly different in the PS group (88.5 [81.3] mm^3 vs 767.5 [368.6] mm^3 [CC group, P = .01], 435.7 [212.2] mm^3 [CS group, P = .001], and 345.1 [116.5] mm^3 [PC group, P = .003]). **C)** Representative immunofluorescence for CD4$^+$ and CD8$^+$ T cells in tumors tissues from the 4 treatment groups. **D, E)** The frequencies of tumor-infiltrating CD4$^+$ cells (**D**) and CD8$^+$ T cells (**E**), shown as mean [SD] number of cells per field (320 × 320 μm square area). **F)** Representative immunofluorescence for the endothelial marker CD31 and the pericyte marker α-SMA in tumor tissues from the 4 treatment groups. **G, H)** Quantification of tumor MVD, shown as area fraction covered by vessels per field (640 × 640 μm square area) (**G**) and mature (pericyte-covered) MVD (**H**), shown as fraction of tumor vessels covered by perivascular cells; error bars represent standard deviations. For autochthonous HCC model data, see Supplementary Figure 2, C-H (available online). Scale bars: 1 mm (**C**) and 200 μm (**F**). P values from log-rank test (**A**) and Wilcoxon rank sum test (**B, D, E, G, H**). All statistical tests were 2-sided. HCC = hepatocellular carcinoma; MVD = microvessel density; SMA = smooth muscle actin.
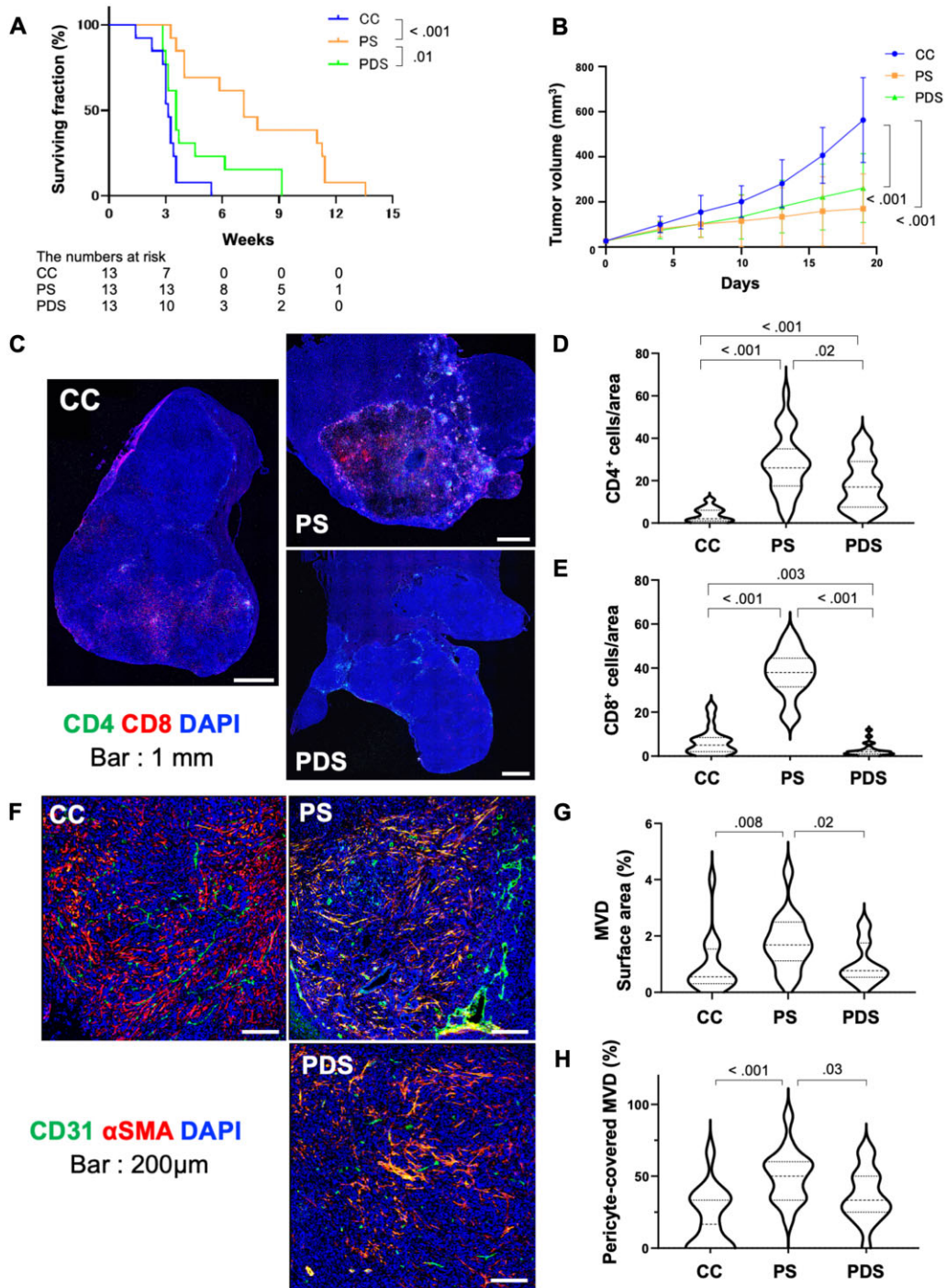
Figure 2. Impact of CD8^{+} T-cell infiltration on the survival benefit of sorafenib after anti–PD-1 therapy priming in orthotopic HCC in mice. **A, B**) Kaplan-Meier survival distributions (**A**) and tumor growth kinetics (**B**) in mice receiving sorafenib with anti-CD8 antibody-mediated depletion (PDS) or immunoglobulin control (PS) after initial anti–PD-1 therapy compared with control (C) (n = 13 mice per treatment group). **C**) Representative immunofluorescence for CD4^{+} and CD8^{+} lymphocytes in tumors tissues from the 3 treatment groups at day 13. **D, E**) The frequencies of intratumoral CD4^{+} (**D**) and CD8^{+} (**E**), shown as mean [SD] number of cells per field (320 × 320 μm square area). (**F**) Representative immunofluorescence for the endothelial marker CD31 and the pericyte marker α-SMA in tumor tissues from the 3 treatment groups at day 13. **G, H**) Quantification of tumor MVD, shown as area fraction covered by vessels per field (640 × 640 μm square area) (**G**) and mature (pericyte-covered) MVD (**H**), shown as fraction of tumor vessels covered by perivascular cells. Scale bars: 1 mm (**C**) and 200 μm (**F**). Error bars represent standard deviations. P values from log-rank test (**A**) and Wilcoxon rank sum test (**B, D, E, G, H**). All statistical tests were 2-sided. HCC = hepatocellular carcinoma; MVD = microvessel density; SMA = smooth muscle actin.

Data Availability

The authors declare that all data supporting the findings of this study are available within the paper and its supplementary material. Raw data are available from the corresponding author upon request.

References

1. Llovet JM, Ricci S, Mazzaferro V, et al. Sorafenib in advanced hepatocellular carcinoma. *N Engl J Med*. 2008;359(4):378–390. doi:10.1056/NEJMoa0708857.

2. Cheng A-L, Kang Y-K, Chen Z, et al. Efficacy and safety of sorafenib in patients in the Asia-Pacific region with advanced hepatocellular carcinoma: a phase III randomised, double-blind, placebo-controlled trial. *Lancet Oncol*. 2009;10(1):25–34. doi:10.1016/s1470-2045(08)70285-7.

3. Bruix J, Qin S, Merle P, et al. Regorafenib for patients with hepatocellular carcinoma who progressed on sorafenib treatment (RESORCE): a randomised, double-blind, placebo-controlled, phase 3 trial. *Lancet*. 2017;389(10064):56–66. doi:10.1016/s0140-6736(16)32453-9.

4. Abou-Alfa GK, Meyer T, Cheng A-L, et al. Cabozantinib in patients with advanced and progressing hepatocellular carcinoma. *N Engl J Med*. 2018;379(1):54–63. doi:10.1056/NEJMoa1717002.

5. Zhu AX, Kang Y-K, Yen C-J, et al. Ramucirumab after sorafenib in patients with advanced hepatocellular carcinoma and increased α-fetoprotein concentrations (REACH-2): a randomised, double-blind, placebo-controlled, phase 3 trial. *Lancet Oncol*. 2019;20(2):282–296. doi:10.1016/s1470-2045(18)30937-9.

6. Kudo M, Finn RS, Qin S, et al. Lenvatinib versus sorafenib in first-line treatment of patients with unresectable hepatocellular carcinoma: a randomised phase 3 non-inferiority trial. *Lancet*. 2018;391(10126):1163–1173. doi:10.1016/s0140-6736(18)30207-1.

7. Chen Y, Ramjiawan RR, Reiberger T, et al. CXCR4 inhibition in tumor microenvironment facilitates anti-programmed death receptor-1 immunotherapy in sorafenib-treated hepatocellular carcinoma in mice. *Hepatology*. 2015;61(5):1591–1602. doi:10.1002/hep.27665.

8. Sia D, Jiao Y, Martinez-Quetglas I, et al. Identification of an immune-specific class of hepatocellular carcinoma, based on molecular features. *Gastroenterol*. 2017;153(3):812–826. doi:10.1053/j.gastro.2017.06.007.

9. Finn RS, Ryoo B-Y, Merle P, et al. Pembrolizumab as second-line therapy in patients with advanced hepatocellular carcinoma in KEYNOTE-240: a randomized, double-blind, phase iii trial. *J Clin Oncol*. 2020;38(3):193–202.

10. Finn RS, Qin S, Ikeda M, et al. Atezolizumab plus bevacizumab in unresectable hepatocellular carcinoma. *N Engl J Med*. 2020;382(20):1894–1905. doi:10.1056/NEJMoa1915745.

11. Ho WJ, Zhu Q, Durham J, et al. Neoadjuvant cabozantinib and nivolumab convert locally advanced hepatocellular carcinoma into resectable disease with enhanced antitumor immunity. *Nat Cancer*. 2021;2(9):891–903., doi:10.1038/s43018-021-00234-4.

12. Fukumura D, Kloepper J, Amoozgar Z, Duda DG, Jain RK. Enhancing cancer immunotherapy using antiangiogenics: opportunities and challenges. *Nat Rev Clin Oncol*. 2018;15(5):325–340. doi:10.1038/nrclinonc.2018.29.

13. Tian L, Goldstein A, Wang H, et al. Mutual regulation of tumour vessel normalization and immunostimulatory reprogramming. *Nature*. 2017;544(7649):250–254. doi:10.1038/nature21724.

14. Shigeta K, Datta M, Hato T, et al. Dual programmed death receptor-1 and vascular endothelial growth factor receptor-2 blockade promotes vascular normalization and enhances antitumor immune responses in hepatocellular carcinoma. *Hepatology*. 2020;71(4):1247–1261. doi:10.1002/hep.30889.

15. Shigeta K, Matsui A, Kikuchi H, et al. Regorafenib combined with PD1 blockade increases CD8 T-cell infiltration by inducing CXCL10 expression in hepatocellular carcinoma. *J Immunother Cancer*. 2020;8(2):e001435. doi:10.1136/jitc-2020-001435.

16. Saint-Jean M, Fronteau C, Peuvrel L, et al. Chemotherapy efficacy after first-line immunotherapy in 18 advanced melanoma patients. *Medicine (Baltimore)*. 2020;99(29):e21329. doi:10.1097/MD.0000000000021329.

17. Schvartsman G, Peng SA, Bis G, et al. Response rates to single-agent chemotherapy after exposure to immune checkpoint inhibitors in advanced non-small cell lung cancer. *Lung Cancer*. 2017;112:90–95. doi:10.1016/j.lungcan.2017.07.034.

18. Saleh K, Daste A, Martin N, et al. Response to salvage chemotherapy after progression on immune checkpoint inhibitors in patients with recurrent and/or metastatic squamous cell carcinoma of the head and neck. *Eur J Cancer*. 2019;121:123–129. doi:10.1016/j.ejca.2019.08.026.

19. Chen Y, Huang Y, Reiberger T, et al. Differential effects of sorafenib on liver versus tumor fibrosis mediated by stromal-derived factor 1 alpha/C-X-C receptor type 4 axis and myeloid differentiation antigen-positive myeloid cell infiltration in mice. *Hepatology*. 2014;59(4):1435–1447. doi:10.1002/hep.26790.

20. Zheng X, Fang Z, Liu X, et al. Increased vessel perfusion predicts the efficacy of immune checkpoint blockade. *J Clin Invest*. 2018;128(5):2104–2115. doi:10.1172/JCI96582.